Compressed sensing radar

Matthew Herman and Thomas Strohmer
Department of Mathematics, University of California
Davis, CA 95616-8633, USA
e-mail: {mattyh,strohmer}@math.ucdavis.edu

***Abstract*—A stylized compressed sensing radar is proposed in which the time-frequency plane is discretized into an N by N grid. Assuming that the number of targets K is small (i.e., $K \ll N^2$), then we can transmit a sufficiently "incoherent" pulse and employ the techniques of compressed sensing to reconstruct the target scene. A theoretical upper bound on the sparsity K is presented. Numerical simulations verify that even better performance can be achieved in practice. By comparing traditional uncertainty principles with those of compressed sensing, this novel approach reveals great potential for better resolution over classical radar.**

***Index Terms*—Compressed sensing, sparse recovery, Alltop sequence.**

I. Introduction

Radar, sonar and similar imaging systems are in high demand in many civilian, military, and biomedical applications. The resolution of these systems is limited by classical time-frequency uncertainty principles. Using the concepts of compressed sensing (CS), we propose a radically new approach to radar. In this simplified version of a monostatic, single-pulse radar system we assume that the targets are radially aligned with the transmitter and receiver.

There are three key points to be aware of: (1) The transmitted signal must be sufficiently "incoherent." Our results rely on the use of a deterministic signal (the Alltop sequence), however, transmitting white noise would yield a similar outcome. (2) This approach does not use a matched filter. (3) The target scene is recovered by exploiting the sparsity constraints.

This report is a first step in formalizing the theory of CS radar and contains many assumptions. In particular, analog to digital (A/D) conversion and related implementation details are ignored.

Throughout this discussion we only consider functions with finite energy; that is, if $f \in L^2(\mathbb{R})$, then $\|f\|_2^2 = \int_{\mathbb{R}} |f(t)|^2 dt < \infty$. The *cross-ambiguity function* for two functions $f, g \in L^2(\mathbb{R})$ is defined as [1]

$$\mathcal{A}_{fg}(\tau,\omega) \;=\; \int_{\mathbb{R}} f(t+\tau/2)\overline{g(t-\tau/2)}\mathrm{e}^{-2\pi \mathrm{i}\omega t}dt \qquad (1)$$

where $\overline{\cdot}$ denotes complex conjugation, and the upright Roman letter $\mathrm{i} = \sqrt{-1}$. The *short-time Fourier transform* (STFT) of f with respect to g is $V_g f(\tau,\omega) = \int_{\mathbb{R}} f(t)\overline{g(t-\tau)}\mathrm{e}^{-2\pi \mathrm{i}\omega t}dt$. A simple change of variable reveals that within a complex factor, the cross-ambiguity function is equivalent to the STFT

$$\mathcal{A}_{fg}(\tau,\omega) \;=\; \mathrm{e}^{\pi \mathrm{i}\omega\tau} V_g f(\tau,\omega). \qquad (2)$$

This work was partially supported by NSF Grant No. DMS-0511461 and NSF VIGRE Grant No. DMS-0135345.

When $f = g$ we have the (self) *ambiguity function* $\mathcal{A}_f(\tau,\omega)$. The shape of the *ambiguity surface* $|\mathcal{A}_f(\tau,\omega)|$ of f is bounded above the *time-frequency plane* (τ,ω) by $|\mathcal{A}_f(\tau,\omega)| \leq \mathcal{A}_f(0,0) = \|f\|_2^2$.

The *radar uncertainty principle* [2] states that if

$$\iint_U |\mathcal{A}_{fg}(\tau,\omega)|^2 d\tau d\omega \;\geq\; (1-\varepsilon)\,\|f\|_2^2\|g\|_2^2 \qquad (3)$$

for some *support* $U \subseteq \mathbb{R}^2$ and $\varepsilon \geq 0$, then $|U| \geq (1-\varepsilon)$. Informally, this can be interpreted as saying that the area of an ambiguity function's "footprint" on the time-frequency plane can only be made so small.

In classical radar, the ambiguity function of f is the main factor in determining the resolution between targets [3]. Therefore, the ability to identify two targets in the time-frequency plane is limited by the essential support of $\mathcal{A}_f(\tau,\omega)$ as dictated by the radar uncertainty principle. The primary result of this paper is that, under certain conditions, CS radar achieves better target resolution than classical radar.

II. Compressed Sensing

Recently, the signal processing/mathematics community has seen a paradigmatic shift in the way information is represented, stored, transmitted and recovered [4], [5], [6]. This area is often referred to as *Sparse Representations and Compressed Sensing*. Consider a discrete signal $\boldsymbol{s}$ of length M (note, boldface variables denote vectors and matrices). We say that it is *K-sparse* if at most $K \ll M$ of its coefficients are nonzero (perhaps under some appropriate change of basis). With this point of view the *true information* content of $\boldsymbol{s}$ lives in at most K dimensions rather than M. In terms of signal acquisition it makes sense then that we should only have to measure a signal $N \sim K$ times instead of M. We do this by observing N *non-adaptive, linear measurements* in the form of $\boldsymbol{y} = \boldsymbol{\Phi s}$, where $\boldsymbol{\Phi}$ is a dictionary of size $N \times M$. If $\boldsymbol{\Phi}$ is sufficiently "incoherent," then the information of $\boldsymbol{s}$ will be embedded in $\boldsymbol{y}$ such that it can be perfectly recovered with high probability. Current reconstruction methods include using greedy algorithms such as *orthogonal matching pursuit* (OMP) [6], and solving the convex problem: $\min \|\boldsymbol{s'}\|_1$ such that $\boldsymbol{\Phi s'} = \boldsymbol{y}$. The latter program is often referred to as *Basis Pursuit* (BP) [4], [5]. A new algorithm, *regularized orthogonal matching pursuit* (ROMP) [7], has recently been proposed which combines the advantages of OMP with those of BP.

1-4244-1539-X/08/$25.00 ©2008 IEEE

III. Matrix Identification via Compressed Sensing

A. Problem Formulation

Consider an unknown matrix $\boldsymbol{H} \in \mathbb{C}^{N\times N'}$ and an orthonormal basis (ONB) $(\boldsymbol{H}_i)_i$ for $\mathbb{C}^{N\times N'}$. Then there exist coefficients $(s_i)_i$ such that

$$\boldsymbol{H} \;=\; \sum_{i=0}^{NN'-1} s_i \boldsymbol{H}_i. \tag{4}$$

Our goal is to identify/discover the coefficients $(s_i)_i$. Since the basis elements are fixed, identifying $(s_i)_i$ is tantamount to discovering $\boldsymbol{H}$. We will do this by designing a test function $\boldsymbol{f} = (f_0, \ldots, f_{N'-1})^{\mathrm{T}} \in \mathbb{C}^{N'}$ and observing $\boldsymbol{Hf} \in \mathbb{C}^N$. Here, $(\,\cdot\,)^{\mathrm{T}}$ denotes the transpose of a vector or a matrix. Figure 1 depicts this from a systems point of view where $\boldsymbol{H}$ is an unknown "block box." Systems like this are ubiquitous in engineering and the sciences. For instance, $\boldsymbol{H}$ may represent an unknown communication channel which needs to be identified for equalization purposes.

$$\boldsymbol{f} \;\longrightarrow\; \boxed{\boldsymbol{H}} \;\longrightarrow\; \boldsymbol{y} = \boldsymbol{Hf}$$
Black Box

Fig. 1. Unknown system $\boldsymbol{H}$ with input probe $\boldsymbol{f}$ and output observation $\boldsymbol{y}$.

For simplicity, from now on assume that $N' = N$. The observation vector can be reformulated as

$$\boldsymbol{y} \;=\; \sum_{i=0}^{N^2-1} s_i \boldsymbol{H}_i \boldsymbol{f} \;=\; \sum_{i=0}^{N^2-1} s_i \boldsymbol{\varphi}_i \;=\; \boldsymbol{\Phi s} \tag{5}$$

where the ith atom $\boldsymbol{\varphi}_i = \boldsymbol{H}_i \boldsymbol{f}$ is a column vector of length N, the concatenation of the atoms $\boldsymbol{\Phi} = (\,\boldsymbol{\varphi}_0 \,|\, \boldsymbol{\varphi}_1 \,|\, \cdots \,|\, \boldsymbol{\varphi}_{N^2-1}\,)$ is an $N \times N^2$ matrix, and $\boldsymbol{s} = (\,s_0,\, s_1,\, \cdots,\, s_{N^2-1}\,)^{\mathrm{T}}$ is a column vector of length N^2. The system of equations in (5) is clearly highly underdetermined. If $\boldsymbol{s}$ is *sufficiently sparse*, then there is hope of recovering $\boldsymbol{s}$ from $\boldsymbol{y}$. To use the reconstruction methods of CS we need to design $\boldsymbol{f}$ so that the dictionary $\boldsymbol{\Phi}$ is *sufficiently incoherent*.

B. The Coherence of a Dictionary

We are interested in how the atoms of a general dictionary $\boldsymbol{\Phi} = (\boldsymbol{\varphi}_i)_i \in \mathbb{C}^{N\times M}$ (with $N \le M$) are "spread out" in $\mathbb{C}^N$. This can be quantified by examining the magnitude of the inner product between its atoms. The *coherence* $\mu(\boldsymbol{\Phi})$ is defined as the maximum of all of the distinct pairwise comparisons $\mu(\boldsymbol{\Phi}) = \max_{i\neq i'} |\langle \boldsymbol{\varphi}_i, \boldsymbol{\varphi}_{i'}\rangle|$. Assuming that each $\|\boldsymbol{\varphi}_i\|_2 = 1$ the coherence is bounded [8], [9] by

$$\sqrt{\frac{M-N}{N(M-1)}} \;\le\; \mu(\boldsymbol{\Phi}) \;\le\; 1. \tag{6}$$

When a dictionary can be expressed as the union of 2 or more ONBs, this lower bound becomes $1/\sqrt{N}$ [10].

C. The Basis of Time-Frequency Shifts

Let the $N \times N$ matrices $\boldsymbol{T}$ and $\boldsymbol{M}$ respectively denote the unit shift and modulation operators where $\boldsymbol{T}(f_0, \ldots, f_{N-2}, f_{N-1})^{\mathrm{T}} = (f_{N-1}, f_0, \ldots, f_{N-2})^{\mathrm{T}}$, $\boldsymbol{M} = \mathrm{diag}\{\omega_N^0, \ldots, \omega_N^{N-1}\}$, and $\omega_N = \mathrm{e}^{2\pi \mathrm{i}/N}$ is the Nth root of unity. The ith time-frequency basis element is defined as

$$\boldsymbol{H}_i \;=\; \boldsymbol{M}^{i \bmod N} \cdot \boldsymbol{T}^{\lfloor i/N \rfloor} \tag{7}$$

where $\lfloor\cdot\rfloor$ is the floor function. A simple calculation shows that the family $(\boldsymbol{H}_i)_{i=0}^{N^2-1}$ forms an ONB with respect to the Frobenius norm. Furthermore, under this basis it is known that some practical systems $\boldsymbol{H}$ with meaningful applications have a sparse representation $\boldsymbol{s}$ [11], [12], [13]. This fact complements the theorems developed in the subsequent sections.

A finite collection of length-N vectors which are time-frequency shifts of a generating vector, and which spans the space $\mathbb{C}^N$ is called a (discrete) *Gabor frame* [2]. Since $(\boldsymbol{H}_i)_{i=0}^{N^2-1}$ forms an ONB, it follow that our dictionary $\boldsymbol{\Phi}$ is a Gabor frame. Without loss of generality assume $\|\boldsymbol{f}\|_2 = 1$. Because each $\boldsymbol{H}_i$ is a unitary matrix we have that $\|\boldsymbol{\varphi}_i\|_2 = 1$ for $i = 0, \ldots, N^2-1$. We can also express $\boldsymbol{\Phi}$ as the concatenation of N blocks

$$\boldsymbol{\Phi} \;=\; \left(\, \boldsymbol{\Phi}^{(0)} \,|\, \boldsymbol{\Phi}^{(1)} \,|\, \cdots \,|\, \boldsymbol{\Phi}^{(N-1)} \,\right) \tag{8}$$

where the kth block $\boldsymbol{\Phi}^{(k)} = \boldsymbol{D}_k \cdot \boldsymbol{W}_N$ with $\boldsymbol{D}_k = \mathrm{diag}\{f_k, \ldots, f_{N-1}, f_0, \ldots, f_{k-1}\}$ and $\boldsymbol{W}_N = (\omega_N^{pq})_{p,q=0}^{N-1}$.

D. The Probing Test Function $\boldsymbol{f}$

We now introduce a candidate probe function $\boldsymbol{f}$ which results in remarkable incoherence properties for the dictionary $\boldsymbol{\Phi}$. Consider the *Alltop sequence* $\boldsymbol{f}_{\mathrm{A}} = (f_n)_{n=0}^{N-1}$ for some prime $N \ge 5$ where [14]

$$f_n \;=\; \frac{1}{\sqrt{N}} \mathrm{e}^{2\pi \mathrm{i} n^3/N}. \tag{9}$$

Let $\boldsymbol{\Phi}_{\mathrm{A}}$ denote the Gabor frame generated by the Alltop sequence (9). Since its atoms are already grouped into $N \times N$ blocks in (8), we will maintain this structure by denoting the jth atom of the kth block as $\boldsymbol{\varphi}_j^{(k)}$. Note that $\|\boldsymbol{f}_{\mathrm{A}}\|_2 = 1$, so we have $0 \le |\langle \boldsymbol{\varphi}_j^{(k)}, \boldsymbol{\varphi}_{j'}^{(k')}\rangle| \le 1$ for any $j, j', k, k' = 0, \ldots, N-1$. Within the *same* block (i.e., $k = k'$) we have

Property 1: $$|\langle \boldsymbol{\varphi}_j^{(k)}, \boldsymbol{\varphi}_{j'}^{(k)}\rangle| \;=\; \begin{cases} 0, & \text{if } j \neq j' \\ 1, & \text{if } j = j'. \end{cases}$$

Thus, each $\boldsymbol{\Phi}^{(k)}$ is an ONB for $\mathbb{C}^N$. Moreover, for *different* blocks (i.e., $k \neq k'$) we have

Property 2: $$|\langle \boldsymbol{\varphi}_j^{(k)}, \boldsymbol{\varphi}_{j'}^{(k')}\rangle| \;=\; \frac{1}{\sqrt{N}}$$

for all $j, j' = 0, \ldots, N-1$. This means that there is a *mutual incoherence* between the atoms of different blocks Trivially, it follows that $\mu(\boldsymbol{\Phi}_{\mathrm{A}}) = 1/\sqrt{N}$. Furthermore, with $M = N^2$ in (6) we see that the lower bound of $1/\sqrt{N+1}$ is *practically attained*. (See [15] for more details on this, mutually unbiased bases (MUBs), and equiangular line sets.)

E. Identifying Matrices via Compressed Sensing: Theory

Having established the incoherence properties of the dictionary $\mathbf{\Phi}_{\mathrm{A}}$ we can now move on to apply the concepts and techniques of CS. It is worth pointing out that most CS scenarios deal with a K-sparse signal $\boldsymbol{s}$ (for some *fixed* K), and one is tasked with determining how many observations are necessary to recover the signal. Our situation is markedly different. Due to the fact that $\mathbf{\Phi}_{\mathrm{A}}$ is constrained to be $N \times N^2$, we know $\boldsymbol{y} = \mathbf{\Phi}_{\mathrm{A}}\boldsymbol{s}$ we will contain exactly N observations. With N fixed, our CS dilemma is to determine how sparse $\boldsymbol{s}$ should be such that it can be recovered from $\boldsymbol{y}$. We hope to recover any K-sparse signal $\boldsymbol{s}$ with $K \leq C \cdot N/\log N$ for some $C > 0$. The following two theorems [15] summarize the recovery of $N \times N$ matrices via CS when identified with the Alltop sequence with prime $N \geq 5$.

Theorem 1: Suppose $\boldsymbol{H} = \sum_i s_i \boldsymbol{H}_i \in \mathbb{C}^{N\times N}$ has a K-sparse representation under the time-frequency ONB, with $K < \frac{1}{2}(\sqrt{N}+1)$, and that we have observed $\boldsymbol{y} = \boldsymbol{H}\boldsymbol{f}_{\mathrm{A}}$. Then we are **guaranteed** to recover $\boldsymbol{s}$ either via BP or OMP.

The sparsity condition in Theorem 1 is rather strict. Instead of the requirement of *guaranteed* perfect recovery, we can ask to achieve it with only *high probability*. This more modest expectation provides us with a much more realistic sparsity condition. Throughout this paper a ***random*** signal refers to a vector or matrix with nonzero coefficients which are independent with a Gaussian distribution of zero mean and unit variance, and which are located according to a uniform distribution.

Theorem 2: Suppose random $\boldsymbol{H} = \sum_i s_i \boldsymbol{H}_i \in \mathbb{C}^{N\times N}$ has a K-sparse representation under the time-frequency ONB where $K \leq N/16\log(N/\varepsilon)$ with $\varepsilon \leq 1/\sqrt{2}$, and that we have observed $\boldsymbol{y} = \boldsymbol{H}\boldsymbol{f}_{\mathrm{A}}$. Then BP will recover $\boldsymbol{s}$ with probability greater than $1 - 2\varepsilon^2 - K^{-\vartheta}$ for some $\vartheta \geq 1$ s.t. $\sqrt{\vartheta \log N/\log(N/\varepsilon)} \leq c$ where c is an absolute constant.

F. Identifying Matrices via Compressed Sensing: Simulation

Numerical simulations were performed and indicate that the theory above is actually quite pessimistic. The simulations were conducted as follows. The values of prime N ranged from 5 to 127, and the sparsity K ranged from 1 to N. For each ordered pair (N, K) a K-sparse vector $\boldsymbol{s}$ of length N^2 was randomly generated. With this random $\boldsymbol{s}$ the observation $\boldsymbol{y} = \mathbf{\Phi}_{\mathrm{A}}\boldsymbol{s}$ was generated. Then, $\boldsymbol{y}$ and $\mathbf{\Phi}_{\mathrm{A}}$ were input to a linear program [16] to solve $\min \|\boldsymbol{s'}\|_1$ s.t. $\mathbf{\Phi}_{\mathrm{A}}\boldsymbol{s'} = \boldsymbol{y}$. This procedure was repeated 15 times and averaged.

Figure 2 shows how the numerical simulations compare to Theorems 1 and 2. The error $\|\boldsymbol{s} - \boldsymbol{s'}\|_2$ as a function of (N, K) is shown as solid, gray-black contour lines. The dashed, red line represents $K = N/\log N$. The zone of "perfect reconstruction" lies *below* this line. In this region random $N \times N$ matrices with $1 \leq K \leq N/\log N$ nonzero entries can be perfectly recovered with high probability. This is empirical evidence that the denominator of K in Theorem 2 can be relaxed from $\log(N/\varepsilon)$ to just $\log N$, and that the proportionality constant $C = 1$. However, it is still an open mathematical problem to prove this for the Alltop sequence. Furthermore, the overly strict constraint of Theorem 1 can be seen by the lower dash-dotted, blue line representing $K = \frac{1}{2}(\sqrt{N}+1)$.

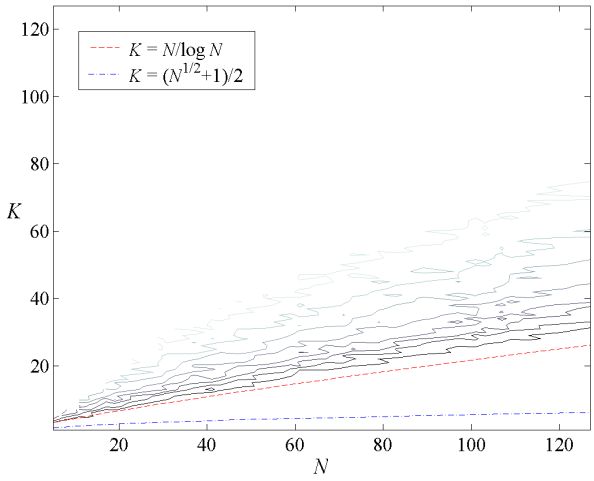

Fig. 2. Matlab simulation of solving $\min \|\boldsymbol{s'}\|_1$ s.t. $\mathbf{\Phi}_{\mathrm{A}}\boldsymbol{s'} = \mathbf{\Phi}_{\mathrm{A}}\boldsymbol{s}$ where $\boldsymbol{s}$ is random. The solid, gray-black lines are the contours of the error $\|\boldsymbol{s} - \boldsymbol{s'}\|_2$ vs. the N-K domain. The dashed, red line shows that Theorem 2 is overly pessimistic. The region below this is the zone of "perfect reconstruction." The lower dash-dotted, blue line illustrates how Theorem 1 is too strict.

IV. Radar

A. Classical Radar Primer

Consider the following simple (narrowband) 1-dimensional, monostatic, single-pulse radar model. *Monostatic* refers to the setup where the transmitter (Tx) and receiver (Rx) are collocated. Suppose a target located at *range* x is traveling with *constant velocity* v and has *reflection coefficient* s_{xv}. Figure 3 shows such a radar with one target. After transmitting signal $f(t)$, the receiver observes the reflected signal

$$r(t) \;=\; s_{xv} f(t - \tau_x) \mathrm{e}^{2\pi \mathrm{i} \omega_v t} \tag{10}$$

where $\tau_x = 2x/c$ is the round trip time of flight, c is the speed of light, $\omega_v \approx -2\omega_0 v/c$ is the Doppler shift, and ω_0 is the carrier frequency. The basic idea is that the *range-velocity* information (x, v) of the target can be inferred from the observed *time delay-Doppler shift* (τ_x, ω_v) of f in (10). Hence, a time-frequency shift operator basis is a natural representation for radar systems [17].

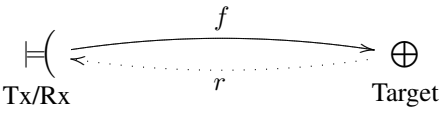

Fig. 3. Simplified radar model. Tx transmits signal f, and Rx receives the reflected (or echoed) signal r according to (10).

Using a **matched filter** at the receiver, the reflected signal r is correlated with a time-frequency shifted version of the

transmitted signal f via the cross-ambiguity function (1)

$$\begin{aligned} |\mathcal{A}_{rf}(\tau,\omega)| &= \Big|\int_{\mathbb{R}} r(t)\overline{f(t-\tau)}\mathrm{e}^{-2\pi\mathrm{i}\omega t}dt\Big| \\ &= |s_{xv}\mathcal{A}_f(\tau-\tau_x,\omega-\omega_v)|. \end{aligned} \quad (11)$$

From this we see that the time-frequency plane consists of the ambiguity surface of f *centered at the target's "location"* (τ_x,ω_v) and scaled by its reflection coefficient $|s_{xv}|$. Extending (11) to include multiple targets is straightforward. Figure 4 illustrates an example of the time-frequency plane with five targets; two of these have overlapping uncertainty regions. The uncertainty region is a rough indication of the essential support of $\mathcal{A}_f$ in (3). Targets which are too close will have overlapping ambiguity functions. This may blur the exact location of a target, or make uncertain how many targets are located in a given region in the time-frequency plane. Thus, the range-velocity resolution between targets of classical radar is limited by the radar uncertainty principle.

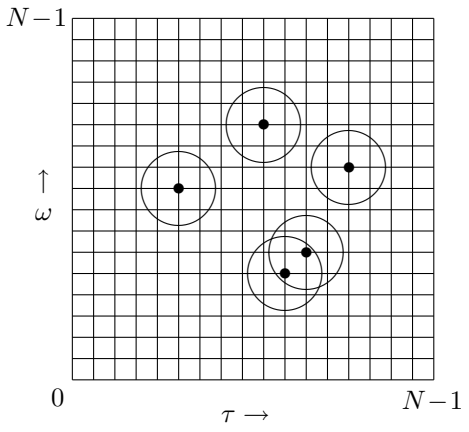

Fig. 4. The time-frequency plane discretized into an $N \times N$ grid. Shown are five targets with their associated uncertainty regions. Classical radar detection techniques may fail to resolve the two targets whose regions are intersecting. In contrast, CS radar will be able to distinguish them as long as the total number of targets is much less then N^2.

B. Compressed Sensing Radar

We now propose our stylized CS radar which under appropriate conditions can "beat" the classical radar uncertainty principle! Consider K targets with unknown range-velocities and corresponding reflection coefficients. Next, discretize the time-frequency plane into an $N \times N$ grid as depicted in Figure 4. Recognizing that each point on the grid represents a unique time-frequency shift $\boldsymbol{H}_i$ (7) (with a corresponding reflection coefficient s_i), it is easy to see that every possible target scene can be represented by some matrix $\boldsymbol{H}$ (4). If the number of targets $K \ll N^2$, then the time-frequency grid will be sparsely populated. By "vectorizing" the grid, we can represent it as an $N^2 \times 1$ **sparse vector** $\boldsymbol{s}$.

Assume that the Alltop sequence is sent by the transmitter[1]. The received signal now is of the form in (5). If the number of targets obey the sparsity constraints in Theorems 1 and 2, then we will be able to reconstruct the original target scene using CS techniques. In reality, we are not actually "beating" the classical uncertainty principle as claimed above. Rather, we are just transferring to a different mathematical perspective. The new *CS uncertainty principle* is dictated by the sparsity constraints of Theorems 1 and 2.

It is interesting to note that Alltop specifically mentions the applicability of his sequence to spread-spectrum radar. The cubic phase in (9) is known in classical radar as a discrete quadratic chirp, which is similar to what bats use to "image" their environment (although bats use a continuous *sonar* chirp). The use of a chirp is an effective way to transmit a wide-bandwidth signal over a relatively short time duration. However, here in CS radar we make use of the incoherence property of the Alltop sequence, which is due to specific properties of prime numbers. Recall the three key points of this novel approach: (1) the transmitted signal must be **incoherent**, (2) there is **no matched filter**, (3) instead, CS techniques are used to recover the **sparse** target scene.

[1]The transmitter in Fig. 3 sends *analog* signals. We assume here that there exists a continuous signal which when discretized is the Alltop sequence (9).

C. Compressed Sensing and Classical Radar Simulations

Figures 5 and 6 show the result of Matlab radar simulations. For purposes of normalization the grid spacing in these figures is $1/\sqrt{N}$. Hence, the numbers shown on the axes represent multiples of $1/\sqrt{N}$. A random time-frequency scene with $K = 10$ targets and $N = 47$ is presented in Figure 5(a). Targets which are darker indicate a larger reflection coefficient. The *CS radar* simulation [16] used the Alltop sequence to identify the targets. In Figure 5(b) it is clear that CS was able to *perfectly reconstruct* the target scene when there was no added noise. Based on the grid of the discretized time-frequency plane in Figure 5 it is obvious that we can resolve targets located at *adjacent grid points*. Thus, **CS radar has a resolution of** $1/2\sqrt{N}$.

Figure 5(c) illustrates how CS starts to suffer in the presence of additive white Gaussian noise (AWGN). Here the signal-to-noise ratio (SNR) is 15 dB. Some faint false positives have appeared, yet the target scene has still been identified. The performance with 5 dB SNR is shown in Figure 5(d). Several targets were lost and many false positives have appeared, which is clearly undesirable. It remains an open problem in the CS community how to deal with such noisy situations.

As a comparison to CS Figure 6 presents *classical radar* reconstruction (which **uses a matched filter** as described in Section IV-A) with two different transmitted pulses. The ambiguity surfaces associated with these two waveforms demonstrate, in some sense, two extremes of traditional radar performance. In the first case, the ambiguity surface is a relatively wide Gaussian pulse, whereas in the second case the ambiguity surface is a highly concentrated "thumbtack" function. We stress that these are not necessarily the final results of traditional target reconstruction, and are included only for rough comparison. In practice, radar engineers use extremely advanced techniques to determine target range and velocity.

Figures 6(a), 6(c), and 6(e) show the original target scene of Figure 5(a) reconstructed using a Gaussian pulse. The (self)

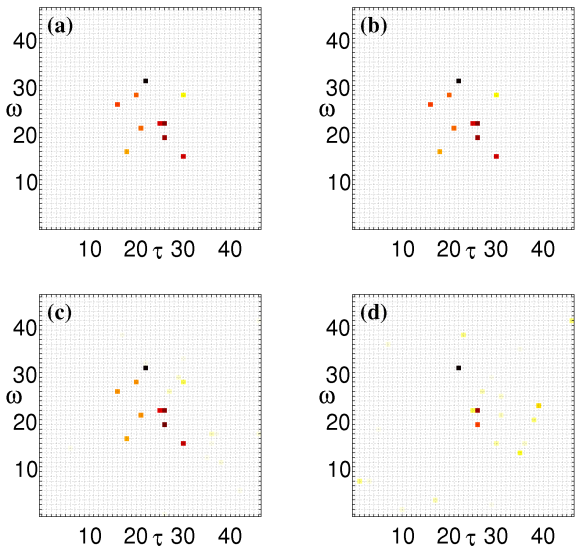

Fig. 5. Radar simulation with $K = 10$ targets on a 47×47 time-frequency grid. (a) Original target scene. CS reconstruction of original target scene with SNR: (b) ∞ dB, (c) 15 dB, (d) 5 dB. Notice CS perfectly recovers (a) in the case of no noise (b).

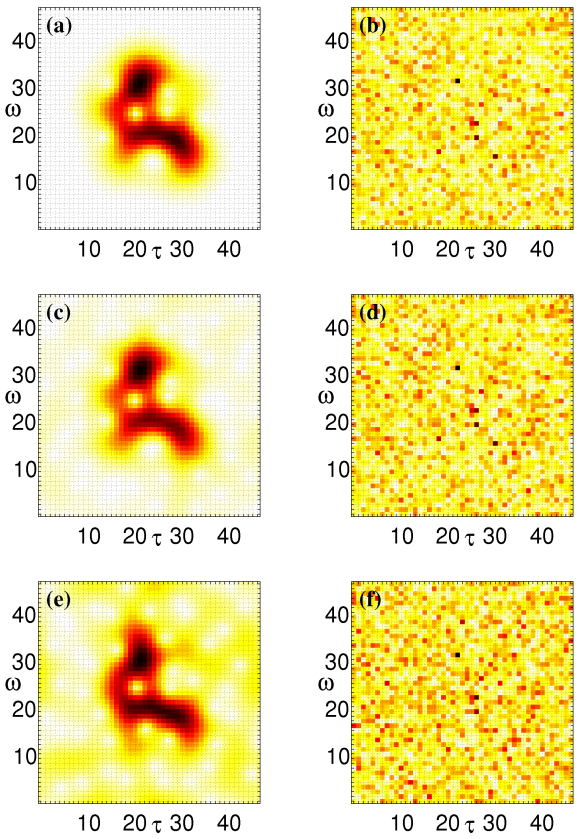

Fig. 6. Traditional radar reconstruction of Fig. 5(a)'s original target scene. With no noise: (a) Gaussian pulse, (b) Alltop sequence. With SNR = 15 dB: (c) Gaussian pulse, (d) Alltop sequence. With SNR = 5 dB: (e) Gaussian pulse, (f) Alltop sequence.

ambiguity function associated with a Gaussian pulse is a two-dimensional Gaussian pulse as a result of the STFT in (2). Therefore, according to (11) we see that the radar scenes in these figures consist of a 2D Gaussian pulse centered at each target in the time-frequency plane. In each of these it is clear that some of the targets are contained within the Heisenberg boxes of neighboring targets. Depending on the sophistication of subsequent algorithms some of the targets (e.g., the two closest in the center) may be unresolvable. It is also clear that Figures 6(c) and 6(e) suffer from added noise, and this compounds the problem of accurate resolution [3].

As a consequence of the grid spacing, the Heisenberg box associated with the Gaussian pulse's ambiguity surface has been normalized to a square of unit area. This is empirically verified in Figures 6(a), 6(c), and 6(e) where we see that the diameter of the uncertainty region around each target spans approximately seven grid points. Since the grid spacing is $1/\sqrt{N}$ we confirm that the base and height of the Heisenberg box are each approximately $7/\sqrt{47} \approx 1$. Therefore, we have a rough measure of the target resolution of a Gaussian pulse: here **classical radar yields a resolution of** $1/2$. Comparing the resolution of classical radar with that of CS we see that $1/2 > 1/2\sqrt{N}$ for $N \geq 2$. Thus, we claim that CS radar can achieve better resolution than classical radar. Moreover, by increasing N the time-frequency plane will be discretized into a finer grid and this will increase CS's resolution. Of course, there are practical limits on how large N can be (e.g., implementation details such as A/D conversion and related hardware issues which we ignore in this paper).

In contrast to a Gaussian pulse we now examine a waveform whose associated ambiguity surface is thumbtack-like. A function is "thumbtack-like" if all of its values are are close to zero except for a unique large spike. Due to Properties 1 and 2 of the Alltop sequence in Section III-D we see that its ambiguity surface has this thumbtack feature. Other thumbtack-like ambiguity surfaces include those associated with the waveforms which generate the equiangular line sets found in [18].

Figures 6(b), 6(d), and 6(f) depict the original target scene *traditionally reconstructed* using the Alltop sequence. Take note of the distinction with compressed sensing radar presented in Section IV-B which also uses this function. Here, the classical approach transmits the Alltop sequence, and then uses a **matched filter** to correlate the received signal with a time-frequency shifted Alltop sequence as in (11). The radar scene will now consist of a thumbtack function centered at each target. In theory, this radar would provide target resolution similar to our CS version (i.e., the target is represented as a point source in time-frequency plane rather than a "spread out" uncertainty region).

However, the situation is not so simple. The non-zero portions of the ambiguity function can accumulate to create undesirable effects. This is shown in Figure 6(b) where it is apparent, *even in the ideal case of no added noise*, that there is a great deal of interference. Moreover, this type of "noise" is deterministic and cannot be remedied by averaging over multiple observations. Notice that the interference seems to be distributed over a wide range of amplitudes. In fact, referring to the original target scene in Figure 5(a), it appears that some of of the weaker targets have been buried in this noise. Even

if a reasonable threshold could be determined, perhaps only the four or five strongest targets would be detected and many false positives would remain.

We present these results to emphasize that naive application of *traditional radar* techniques with the Alltop sequence will fail if the radar scene contains more than just a few strong targets. The outcome will be similar if other low-correlation sequences are used.

Regardless of whether a transmitted waveform has an ambiguity surface which is spread or narrow, interference from adjacent targets will necessarily occur in classical radar, and this will result in undesirable effects. In contrast, CS radar does not experience this interference since it completely dispenses with the need for a matched filter. Therefore, there are no issues with the ambiguity function of the transmitted signal.

V. Discussion

We have provided a sketch for a high-resolution radar system based on CS. Assuming that the number of targets obey the sparsity constraint in Theorem 2, the Alltop sequence will perfectly identify the radar scene with high probability using CS techniques. Numerical simulations confirm that this sparsity constraint is too strict and can be relaxed to $K \leq N/\log N$, although this has yet to be proven mathematically.

It must be emphasized that our model presents radar in an overly simplified manner. In reality, radar engineers employ highly sophisticated methods to identify targets. For example, rather than a single pulse, a signal with multiple pulses is often used and information is averaged over several observations. We also did not address how to discretize the analog signals used in both CS and classical radar. A more detailed study addressing these issues is the topic of another paper.

Related to the discretization issue is the fact that CS radar does not use a matched filter at the receiver. This will directly impact A/D conversion, and has the potential to reduce the overall data rate and to simplify hardware design. These matters are discussed in [19], although it does not consider the case of moving targets. In our study the major benefit of relinquishing the matched filter is to avoid the target uncertainty and interference resulting from the ambiguity function.

Since many of the implementation details of our CS radar have yet to be determined, and since classical radar can also be implemented in many ways we were only able to make a rough comparison between their respective resolutions. *Regardless, the radar uncertainty principle lies at the core of traditional approaches and limits their performance.* We contend that CS provides the potential to achieve higher resolution between targets. The radar simulations presented confirm this claim.

It must be stressed again that the success of this stylized CS radar relied on the incoherence of the dictionary $\mathbf{\Phi}_{\mathrm{A}}$ resulting from the Alltop sequence. There exist other probing functions with similar incoherence properties. Numerical simulations with $\boldsymbol{f}$ as a random Gaussian signal, as well as a constant-envelope random-phase signal indicate similar behavior to what we have reported for the Alltop sequence. At the time of writing this paper we became aware of a similar study [20] where the properties of these functions are analyzed in the context of CS. There is also the possibility of combining classical radar techniques with ℓ_1 recovery. Initial tests show that while we get good reconstruction, the results are not guaranteed, even in the case of no noise.

Narrowband radar is by no means the only application to which the techniques presented here can be used. *Wideband* radar admits a received signal which is well-represented by a wavelet basis, and the dictionary $\mathbf{\Phi}$ could be reformulated accordingly. There are also applications to many other linear time-varying systems such as sonar, estimation of underwater acoustic communication channels [12], and blind source separation [13].

References

[1] R. E. Blahut, "Theory of remote surveillance algorithms," in *Radar and Sonar, Part I*, ser. IMA Volumes in Mathematics and its Aplications, R. E. Blahut, W. Miller Jr., and C. H. Wilcox, Eds. NY: Springer-Verlag, 1991, vol. 32, pp. 1–65.

[2] K. Gröchenig, *Foundations of time-frequency analysis*. Boston: Birkhäuser, 2001.

[3] A. W. Rihaczek, *High-Resolution Radar*. Boston: Artech House, 1996, (originally published: McGraw-Hill, NY, 1969).

[4] D. L. Donoho, "Compressed sensing," *IEEE Trans. Inf. Theory*, vol. 52, no. 4, pp. 1289–1306, 2006.

[5] E. J. Candès, J. Romberg, and T. Tao, "Robust uncertaitny principles: Exact signal reconstruction from highly incomplete frequency information," *IEEE Trans. Inf. Theory*, vol. 52, no. 2, pp. 489–509, Feb. 2006.

[6] J. A. Tropp, "Greed is good: Algorithmic results for sparse approximation," *IEEE Trans. Inf. Theory*, vol. 50, no. 10, pp. 2231–2242, Oct. 2004.

[7] D. Needell and R. Vershynin, "Uniform uncertainty principle and signal recovery via regularized orthogonal matching pursuit," July 2007, preprint.

[8] R. A. Rankin, "The closest packing of spherical caps in n dimensions," *Proc. Glasgow Math. Assoc.*, vol. 2, pp. 139–144, 1955.

[9] L. R. Welch, "Lower bounds on the maximum cross-correlation of signals," *IEEE Trans. Inf. Theory*, vol. 20, no. 3, pp. 397–399, 1974.

[10] P. Delsarte, J. M. Goethals, and J. J. Seidel, "Bounds for systems of lines and Jacobi poynomials," *Philips Res. Repts*, vol. 30, no. 3, pp. 91*–105*, 1975, issue in honour of C.J. Bouwkamp.

[11] P. A. Bello, "Characterization of randomly time-variant linear channels," *IEEE Trans. on Comm.*, vol. 11, no. 4, pp. 360–393, Dec. 1963.

[12] W. Li and J. C. Preisig, "Estimation and equalization of rapidly varying sparse acoustic communication channels," *Proc. IEEE OCEANS 2006*, pp. 1–6, Sept. 2006.

[13] Z. Shan, J. Swary, and S. Aviyente, "Underdetermined source separation in the time-frequency domain," *Proc. IEEE ICASSP 2007*, pp. 945–948, April 2007.

[14] W. O. Alltop, "Complex sequences with low periodic correlations," *IEEE Trans. Inf. Theory*, vol. 26, no. 3, pp. 350–354, May 1980.

[15] M. Herman and T. Strohmer, "High-resolution radar via compressed sensing," *Sub. to IEEE Trans. Sig. Proc.*, Oct. 2007.

[16] M. Grant, S. Boyd, and Y. Ye, "cvx: Matlab software for disciplined convex programming." [Online]. Available: `http://www.stanford.edu/~boyd/cvx/`

[17] L. Auslander and R. Tolimieri, "Radar ambiguity functions and group theory," *SIAM Journal on Mathematical Analysis*, vol. 16, no. 3, pp. 577–601, 1985.

[18] S. D. Howard, A. R. Calderbank, and W. Moran, "The finite Heisenberg-Weyl groups in radar and communications," *EURASIP Journal on Applied Signal Processing*, vol. 2006, pp. 1–12, article ID 85685.

[19] R. Baraniuk and P. Steeghs, "Compressive radar imaging," *Proc. 2007 IEEE Radar Conf.*, pp. 128–133, Apr. 2007.

[20] G. E. Pfander, H. Rauhut, and J. Tanner, "Identification of matrices having a sparse representation," preprint June 2007.